

Effects of molecular beam epitaxy growth conditions on composition and optical properties of $\text{In}_x\text{Ga}_{1-x}\text{Bi}_y\text{As}_1$

Y. Zhong, P. B. Dongmo, J. P. Petropoulos, and J. M. O. Zide

Citation: [Applied Physics Letters](#) **100**, 112110 (2012); doi: 10.1063/1.3695066

View online: <http://dx.doi.org/10.1063/1.3695066>

View Table of Contents: <http://scitation.aip.org/content/aip/journal/apl/100/11?ver=pdfcov>

Published by the [AIP Publishing](#)

Articles you may be interested in

[Carrier localization and in-situ annealing effect on quaternary \$\text{Ga}_1\text{xIn}_x\text{As}_y\text{Sb}_1\text{y}/\text{GaAs}\$ quantum wells grown by Sb pre-deposition](#)

Appl. Phys. Lett. **102**, 113101 (2013); 10.1063/1.4795866

[Temperature dependence of \$E_0\$ and \$E_0 + SO\$ transitions in \$\text{In}_{0.53}\text{Ga}_{0.47}\text{Bi}_x\text{As}_{1-x}\$ alloys studied by photoreflectance](#)

J. Appl. Phys. **112**, 113508 (2012); 10.1063/1.4768262

[Role of native defects in nitrogen flux dependent carrier concentration of InN films grown by molecular beam epitaxy](#)

J. Appl. Phys. **112**, 073510 (2012); 10.1063/1.4757031

[Molecular beam epitaxial growth and optical properties of highly mismatched \$\text{ZnTe}_{1-x}\text{O}_x\$ alloys](#)

Appl. Phys. Lett. **100**, 011905 (2012); 10.1063/1.3674310

[Molecular-beam epitaxy of phosphor-free 1.3 \$\mu\text{m}\$ InAlGaAs multiple-quantum-well lasers on InP \(100\)](#)

J. Vac. Sci. Technol. B **25**, 1090 (2007); 10.1116/1.2737434



AIP | Journal of Applied Physics

Journal of Applied Physics is pleased to announce **André Anders** as its new Editor-in-Chief

Effects of molecular beam epitaxy growth conditions on composition and optical properties of $\text{In}_x\text{Ga}_{1-x}\text{Bi}_y\text{As}_{1-y}$

Y. Zhong,¹ P. B. Dongmo,¹ J. P. Petropoulos,² and J. M. O. Zide^{1,a)}

¹Department of Materials Science and Engineering, University of Delaware, Newark, Delaware 19716, USA

²Department of Electrical and Computer Engineering, University of Delaware, Newark, Delaware 19716, USA

(Received 11 January 2012; accepted 28 February 2012; published online 16 March 2012)

We describe the growth conditions of $\text{In}_x\text{Ga}_{1-x}\text{Bi}_y\text{As}_{1-y}$ (lattice-mismatched and matched) on InP substrates by molecular beam epitaxy and the resulting properties. Due to their anomalously narrow bandgaps and the presence of bismuth, these materials are promising for optoelectronics and thermoelectrics. Low growth temperature and moderate As/Bi beam equivalent pressure ratios are beneficial for Bi incorporation, in good qualitative agreement with $\text{GaBi}_y\text{As}_{1-y}$ on GaAs. Up to 6.75% bismuth is incorporated. High resolution x-ray diffraction and reciprocal space mapping show that $\text{In}_x\text{Ga}_{1-x}\text{Bi}_y\text{As}_{1-y}$ samples exhibit good crystalline quality and zero relaxation. The band gap is reduced in agreement with theoretical predictions. Lattice-matched samples have been produced with lattice mismatch $\leq 0.21\%$. © 2012 American Institute of Physics. [<http://dx.doi.org/10.1063/1.3695066>]

Dilute bismuthides (i.e., III-V semiconductors containing small amounts of bismuth in the alloy) are a relatively new class of materials which possess many interesting properties. Due to valence band anticrossing (VBAC),¹ the incorporation of Bi into GaAs or $\text{In}_{1-x}\text{Ga}_x\text{As}$ will result in anomalously narrow bandgaps, which has potential application in mid-infrared (mid-IR) optoelectronics.^{2,3} Additionally, dilute bismuthides are expected to be a good thermoelectric material because of their combination of low thermal conductivity and high power factor. Previous research focus on the growths and properties of $\text{GaBi}_x\text{As}_{1-x}$, with the incorporation of Bi up to 13%.^{2,4-6} However, the growth of lattice-matched materials, which are preferable for optoelectronics, cannot be achieved using $\text{GaBi}_x\text{As}_{1-x}$ on GaAs. In contrast, the growth of the quaternary alloy $\text{In}_x\text{Ga}_{1-x}\text{Bi}_y\text{As}_{1-y}$ lattice-matched on InP is possible. Previously, there have been reports of lattice-mismatched $\text{In}_x\text{Ga}_{1-x}\text{Bi}_y\text{As}_{1-y}$ on InP with limited study of growth conditions.⁷⁻⁹ More recently, bandgap narrowing has been observed and modeled in lattice-mismatched materials.³ In this letter, we elucidate the influence of variables such as Bi/As beam equivalent pressure (BEP) ratio and substrate temperature on Bi concentration in materials grown by molecular beam epitaxy (MBE). We also exhibit the effects of composition on bandgap. In addition, we demonstrate the growth of nominally lattice-matched materials and describe their optical properties.

$\text{In}_x\text{Ga}_{1-x}\text{Bi}_y\text{As}_{1-y}$ samples were grown on (001) oriented InP:Fe substrates in a III-V solid source MBE system, equipped with effusion cells for In, Ga, and Bi, and a two-zone valved cracker source for As_2 . The substrate temperature is monitored by measuring the temperature-dependence of the substrate band edge, and BEP is measured using an ionization gauge. The native oxide on the InP substrate is desorbed under an As overpressure of 1.0×10^{-5} Torr. The substrate temperature is then reduced to 250–330 °C and the

As BEP is reduced to 2.0×10^{-6} Torr. A 50–70 nm buffer layer $\text{In}_{0.53}\text{Ga}_{0.47}\text{As}$ is first deposited onto the substrate to provide a clean epitaxial surface. Then, the film layer $\text{In}_{0.53}\text{Ga}_{0.47}\text{Bi}_y\text{As}_{1-y}$ with various Bi BEPs (ranging from 1.0×10^{-8} to 3.0×10^{-8} Torr) is grown. During all growths, the reflection high energy electron diffraction (RHEED) displays clear 2×4 patterns.

Figure 1 shows ω - 2θ high-resolution x-ray diffraction (HR-XRD) scans using Cu K α l radiation for three $\text{In}_x\text{Ga}_{1-x}\text{Bi}_y\text{As}_{1-y}$ samples along the (004) direction. The sharp peak at 31.6682° represents the substrate peak, and the peak at a smaller angle corresponds to the $\text{In}_x\text{Ga}_{1-x}\text{Bi}_y\text{As}_{1-y}$ film peak, which proves lattice constant increase brought by the incorporation of large bismuth atoms. The broad bump between the substrate peak and the film peak comes from the modulation of the buffer layer $\text{In}_{0.53}\text{Ga}_{0.47}\text{As}$ which is much thinner than the film. Indium concentration varies by approximately $\pm 2\%$. All of these curves show the existence of thickness fringes, indicating our samples have very smooth epitaxial interfaces and reasonable good crystalline quality.

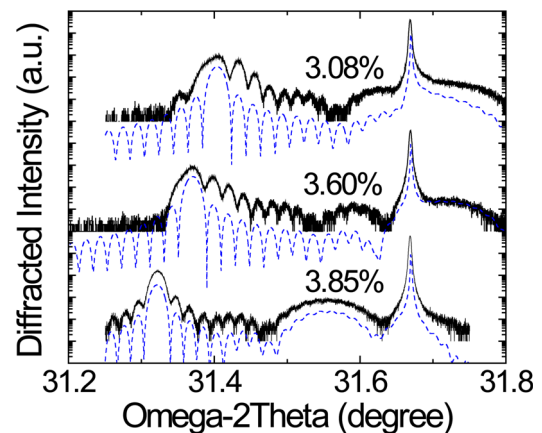


FIG. 1. (Color online) HR-XRD (004) ω - 2θ scans for $\text{In}_x\text{Ga}_{1-x}\text{Bi}_y\text{As}_{1-y}$ epilayers on InP (black lines) with Bi content of 3.08%, 3.60%, and 3.85% (RBS). The blue lines are simulations.

^{a)}Electronic mail: zide@udel.edu.

The samples in this figure are grown at 255 °C (3.85%), 285 °C (3.60%), and 300 °C (3.09%). Generally, we observe Bi concentration increasing when the growth temperature decreases, as shown by the film peak moving to lower angles. Despite this trend, the determination of Bi content from ω - 2θ scans directly is not ideal due to the indium concentration variation, which is displayed by deviation of the buffer layer peak position. Also, the incorporation of large Bi atoms into $\text{In}_{1-x}\text{Ga}_x\text{As}$ will lead to lattice dilation, rendering the expected lattice constants of InAs, GaAs, InBi, and GaBi to be no longer applicable. Therefore, ω - 2θ scans alone are not a reliable method to determine Bi concentration. In this letter, we instead use Rutherford backscattering spectrometry (RBS) measurements in combination with HR-XRD ω - 2θ scans to determine Bi concentration.

RBS is ideal to quantitatively analyze Bi concentration because of its high sensitivity to heavy elements like bismuth. Figure 2 shows randomly oriented and aligned RBS spectra (as well as a simulation) of $\text{In}_{0.49}\text{Ga}_{0.51}\text{Bi}_{0.03}\text{As}_{0.97}$ directly deposited on an InP substrate. The individual contributions of In, Ga, As, P, and Bi are indicated in the simulation. The high crystalline quality of this sample is demonstrated by the much lower yield in the aligned spectrum than the random spectrum. There is no peak shown up on the aligned spectrum, which indicates that almost all Bi atoms incorporate substitutionally instead of occupying the interstitial sites. As shown in the figure, the Bi signal is clearly separated from the others, and the concentration can, therefore, easily be determined.

To explore the Bi incorporation conditions, we completed two series of growths. In the first series, growth temperature is the variable while all other conditions are kept constant. The total film thickness for each sample is 280 nm, and the growth rate is 485 nm/h. In the second series, the Bi BEP is varied instead. The total film thickness is 450 nm, and the growth rate is around 615 nm/h. Figure 3(a) shows Bi concentration as a function of growth temperature. Generally, Bi content increases with decreased growth temperature and reaches a plateau when the growth temperature is below 285 °C. Figure 3(b) indicates Bi concentration dependence on various Bi BEPs. Bi concentration gradually increases with higher Bi BEPs, and the highest Bi content (average

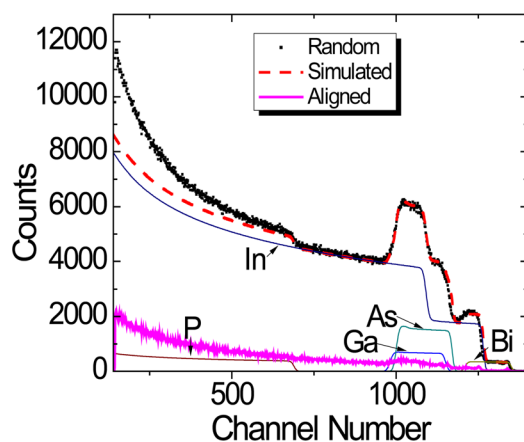


FIG. 2. (Color online) Randomly oriented, simulated, and aligned RBS spectrum for $\text{In}_{0.49}\text{Ga}_{0.51}\text{Bi}_{0.03}\text{As}_{0.97}$ epilayers. Components of In, Ga, Bi, As, and P are indicated based on simulation.

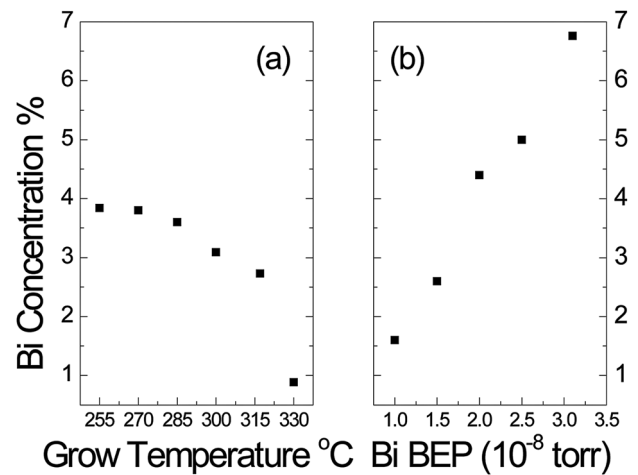


FIG. 3. Effects of growth conditions on bismuth incorporation in $\text{In}_x\text{Ga}_{1-x}\text{Bi}_y\text{As}_{1-y}$. (a) Bi content dependence on growth temperature. (b) Bi content dependence on Bi BEP.

value because this sample has Bi concentration gradient) reaches 6.75%. Bi droplets, which imply that it is more difficult for Bi to incorporate, begin to appear when the growth temperature is above 285 °C or Bi BEP is above 2.0×10^{-8} Torr. From the scanning electron microscope-energy dispersive spectroscopy (SEM-EDS) results, the Bi droplets are separated into two phases, and one side of the droplets contains much higher Bi concentration than the other side. This finding agrees with the previous report.¹⁰ At Bi BEP of 3.1×10^{-8} Torr, Bi concentration distribution in the growth direction, which is demonstrated by the inclined shape of Bi signal in the RBS spectrum shown in Figure 4. We found a linear Bi concentration increase of 0.0625% Bi/nm, or Bi concentration ranging from 1.4% near the buffer layer to 14.4% near the surface, though the resolution of RBS measurements is insufficient to determine if the concentration profile is actually linear. The existence of Bi concentration gradient is indicating that a Bi floating layer is

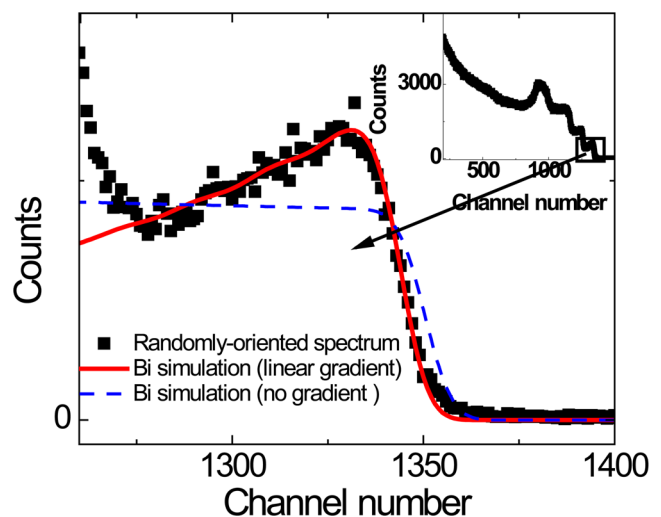


FIG. 4. (Color online) Detail of the large-mass edge of the randomly oriented (black dots) RBS spectrum for $\text{In}_{0.54}\text{Ga}_{0.46}\text{Bi}_{0.0675}\text{As}_{0.9325}$, the whole spectrum is in the inset. Red line is the simulation for Bi signal with an approximately linear Bi concentration gradient of about 0.0625%/nm in the growth direction. Blue line is a conventional fitting with a constant Bi concentration which clearly does not fit these data.

forming on the surface; consequently, it becomes very difficult for Bi to incorporate, and this is close to the highest Bi limit in the given growth conditions. Overall, the Bi incorporation trends agree qualitatively with what has been observed in $\text{GaBi}_x\text{As}_{1-x}$ growths,^{2,4} though specific parameters vary.

The band gap of these films, shown in Figure 5, is measured using a PerkinElmer Lambda 750 UV/VIS. The theoretical values are calculated using the VBAC model as reported previously.³ We did not account for the strain effect because currently it is not accessible in this material system. As expected, the incorporation of Bi leads to a reduction in band gap. In related work, it has been shown that the bandgap narrowing occurs mainly in the valence band.¹¹ The long wavelength limit of our $\text{In}_x\text{Ga}_{1-x}\text{Bi}_y\text{As}_{1-y}$ measured from experiment is 2755 nm, which is the highest reported to date. As it is proven by the HR-XRD and RBS measurements, there are small variations in the In/Ga ratio which will affect the actual bandgap. We show three simulation lines with different In concentrations in varied colors and include the experimental measurements in the corresponding color. The experimental results agree reasonably well with the model; the scatter in the data might result from defects.

These samples are lattice-mismatched alloys. The degree of relaxation is, therefore, an important concern because dislocations resulting from relaxation can significantly affect the related material properties. Reciprocal space mapping (RSM) is used to study strain and relaxation. The asymmetric RSM scan along (224) direction for $\text{In}_{0.520}\text{Ga}_{0.480}\text{Bi}_{0.036}\text{As}_{0.964}$ is shown in Figure 6. The horizontal and vertical axes represent the parallel (110) and normal (001) directions with respect to the sample's surface. The upper and lower peaks originate from InP substrate and $\text{In}_{0.520}\text{Ga}_{0.480}\text{Bi}_{0.036}\text{As}_{0.964}$ film, respectively. As shown in the figure, the two peaks have the same horizontal coordinate, indicating the film is 100% strained. The series of peaks along (001) are thickness fringes, which also confirm the good crystalline quality of our sample and especially the interface. The broadening of the film peak along ω scan direction could be due to either wafer curvature or

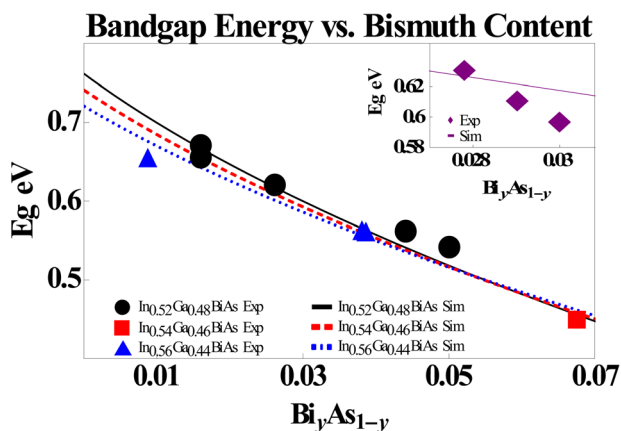


FIG. 5. (Color online) Lines represent simulation results (predicted from VBAC model) and marks represent experimental gap energies of $\text{In}_x\text{Ga}_{1-x}\text{Bi}_y\text{As}_{1-y}$ as a function of Bi concentration. Black circle, red square, and blue triangle indicate different In concentrations which are shown in the legend. Inset: Theoretical (line) and experimental (diamonds) results of nominally lattice-matched samples band gap values.

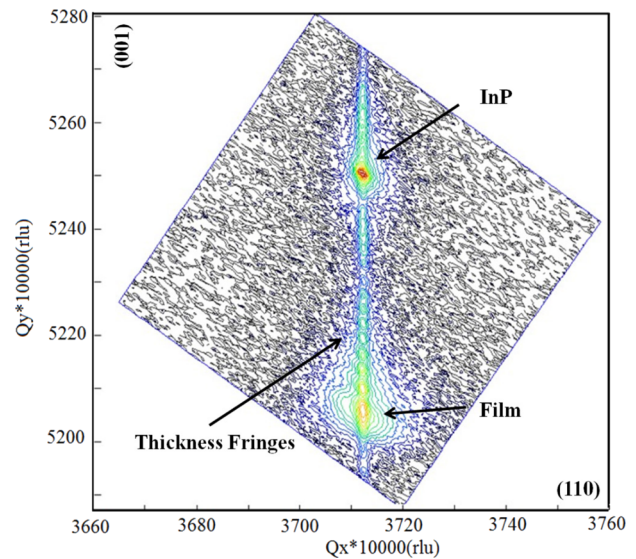


FIG. 6. (Color online) A typical (224) reciprocal space map for $\text{In}_{0.52}\text{Ga}_{0.48}\text{Bi}_{0.036}\text{As}_{0.964}$. The Q_x and Q_y represent the directions that are parallel and normal to the sample's surface. Intensities are on a log scale.

dislocation-induced tilt/twist.¹² Interestingly, this fully strained sample's thickness is 280 nm, which is much larger than the critical thickness 69 nm predicted from a simplified Matthews-Blakeslee model,¹³ which assumes the epilayer and substrate are isotropic elastic materials. This has been observed in other low-temperature-grown systems as well.¹⁴ One possible explanation is the growth condition (low temperature) is far from the thermodynamic equilibrium, and strain release requires excess thermal energy¹⁵ to permit dislocation motion. Alternatively, defect nucleation could be insufficient to permit relaxation.

For the growths of nominally lattice-matched samples, we decrease the In/Ga ratio based on the RBS and HR-XRD results to compensate the lattice constant increase brought by Bi. We report the growth of three nominally lattice-matched samples at different growth temperatures 285 °C, 300 °C, and 317 °C with corresponding Bi concentration of 3.00%, 2.90%, and 2.78% (as determined by RBS). The film thickness for each is 260 nm, and the growth rate is 548 nm/hr. All films are directly deposited onto the substrate without a buffer layer. The ω -2 θ scans of the three samples from HR-XRD are shown in Figure 7(a). The sharp tall peak is InP substrate peak; the small peak adjacent to it is the film $\text{In}_x\text{Ga}_{1-x}\text{Bi}_y\text{As}_{1-y}$. From Vegard's law, we can calculate the lattice mismatches of the three samples to be 0.21% (3.00% Bi), 0.10% (2.90% Bi), and 0.08% (2.78%), which is quite close to lattice-matched. Figures 7(b) and 7(c) exhibit the (224) RSM scan for the sample with 3.00% Bi and the (004) RSM scan for the sample with 2.78% Bi. These RSM scans further confirmed our samples are effectively lattice-matched. The band gaps of these samples are around 0.6 eV. Thus, films with wavelength above 2 μm have been demonstrated with negligible lattice mismatch. As shown in the inset in Figure 5, the theoretical model for bandgap of lattice-matched materials does not agree well with measurements. This is because there is a fitting parameter in our model that is determined by the interacting-strength matrix elements, which requires calculation from the experimental

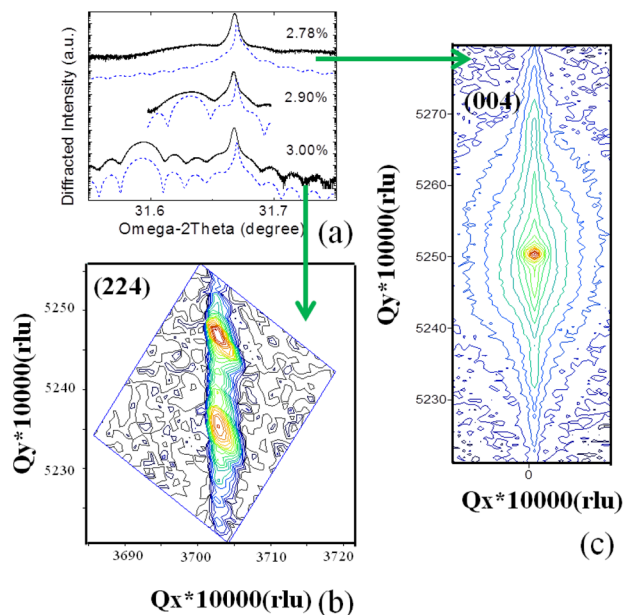


FIG. 7. (Color online) (a) HR-XRD (004) ω - 2θ scans for nominally lattice-matched $\text{In}_x\text{Ga}_{1-x}\text{Bi}_y\text{As}_{1-y}$ epilayers on InP (black lines) with Bi content of 2.78%, 2.90%, and 3.00% (RBS) (top to bottom). The blue lines are simulations. (b) (224) RSM of nominally lattice-matched sample with 3.00% Bi. (c) (004) RSM of nominally lattice-matched sample with 2.78% Bi.

data. It suggests the need for further refinement of our model once more data are available. The effects of strain, which are not well-explored for these materials, are also neglected. Based on the experiment results, $\text{In}_x\text{Ga}_{1-x}\text{Bi}_y\text{As}_{1-y}$ holds great promise for application in mid-IR devices.

In conclusion, we have determined the effects of growth conditions of $\text{In}_x\text{Ga}_{1-x}\text{Bi}_y\text{As}_{1-y}$ on composition and resulting optical properties. Low growth temperature and appropriate Bi/As flux ratio are required to maximize Bi incorporation. Good crystalline quality, smooth interfaces, and zero relaxation are confirmed by the HR-XRD. Up to 6.75%, Bi is substitutionally incorporated into the film

(based on the RBS measurement), and the corresponding wavelength of this sample is $2.7\ \mu\text{m}$. We have also grown nominally lattice-matched samples with lattice mismatch $\leq 0.21\%$, and the wavelengths of these samples are all above $2\ \mu\text{m}$.

The authors wish to thank Steven Hegedus and Zhan Shu at the Institute for Energy Conversion (University of Delaware) for help with spectrophotometry as well as Leszek Wielunski at the Rutgers University for the RBS measurements. Finally, the authors wish to acknowledge the Office of Naval Research for financial support through the Young Investigator Program and additional seedling funding.

¹T. Tiedje, E. C. Young, and A. Mascarenhas, *Int. J. Nanotechnol.* **5**, 963 (2008).

²X. Lu, D. A. Beaton, R. B. Lewis, T. Tiedje, and M. B. Whitwick, *Appl. Phys. Lett.* **92**, 192110 (2008).

³J. P. Petropoulos, Y. Zhong, and J. M. O. Zide, *Appl. Phys. Lett.* **99**, 031110 (2011).

⁴M. Yoshimoto, S. Murata, A. Chayahara, Y. Horino, J. Saraie, and K. Oe, *Jpn. J. Appl. Phys.* **42**, L1235 (2003).

⁵A. G. Norman, R. France, and A. J. Ptak, *J. Vac. Sci. Technol. B* **29**, 03C121 (2011).

⁶R. N. Kini, L. Bhusal, A. J. Ptak, R. France, and A. Mascarenhas, *J. Appl. Phys.* **106**, 043705 (2009).

⁷G. Feng, K. Oe, and M. Yoshimoto, *Phys. Status Solidi A* **203**, 2670 (2006).

⁸G. Feng, K. Oe, and M. Yoshimoto, *J. Cryst. Growth* **301–302**, 121 (2007).

⁹G. Feng, M. Yoshimoto, K. Oe, A. Chayahara, and Y. Horino, *Jpn. J. Appl. Phys.* **44**, L1161 (2005).

¹⁰G. Vardar, M. V. Warren, M. Kang, S. Jeon, and R. S. Goldman, presented at the 28th North American Molecular Beam Epitaxy Conference, San Diego, CA, 2011.

¹¹R. Kudrawiec, J. Kopaczek, J. Misiewicz, J. P. Petropoulos, Y. Zhong, and J. M. O. Zide, *Appl. Phys. Lett.* **99**, 251906 (2011).

¹²M. A. Moram and M. E. Vickers, *Rep. Prog. Phys.* **72**, 036502 (2009).

¹³J. W. Matthews and A. E. Blakeslee, *J. Cryst. Growth* **27**, 118 (1974).

¹⁴R. J. Hauenstein, B. M. Clemens, R. H. Miles, O. J. Marsh, E. T. Croke, and T. C. McGill, *J. Vac. Sci. Technol. B* **7**, 767 (1989).

¹⁵J. Y. Tsao, B. W. Dodson, S. T. Picraux, and D. M. Cornelison, *Phys. Rev. Lett.* **59**, 2455 (1987).